

The Mechanism of Synchronization in a Random Dynamical System

Dong-Uk Hwang,^{1,2,a} Inbo Kim,^{1,2,b} Sunghwan Rim,^{1,c} Chil-Min Kim,^{1,d} and Young-Jai Park^{2,e}

¹*National Creative Research Initiative Center for Controlling Optical Chaos,
Department of Physics, Paichai University, Seogu, Daejeon 302-735, Korea*

²*Department of Physics and Basic Science Research Institute,
Sogang University, Seoul 100-611, Korea*

(December 19, 2019)

The mechanism of synchronization in the random Zaslavsky map is investigated. From the error dynamics of two particles, the structure of phase space was analyzed, and a transcritical bifurcation between a saddle and a stable fixed point was found. We have verified the structure of on-off intermittency in terms of a biased random walk. Furthermore, for the generalized case of the ensemble of particles, a *modified definition* of the size of a snapshot attractor was exploited to establish the link with a random walk. As a result, the structure of on-off intermittency in the ensemble of particles was explicitly revealed near the transition.

PACS numbers: 05.40.-a, 05.45.Xt

the random jumping behavior persists permanently, so the concept of attractor is inappropriate. Hence, after transient times had elapsed, they took a snapshot of the particle distribution on the fluid surface, and called it *a snapshot attractor* [1,3]. They observed that the long-time particle distribution that evolves from an initial smooth distribution exhibits an “extreme form of temporally intermittent bursting” on the chaotic side near the transition.

After YOC’s work, a type of intermittent behavior known as on-off intermittency has been reported by Platt, Speigel and Tresser [4]. On-off intermittency refers to the situation where some dynamical variables exhibit two distinct states in their course of time evolution. One is the ‘off’ state, where the variable remain approximately a constant, and the other is the ‘on’ state, where the variable temporarily burst out of the off state. It has long been thought that the intermittent behavior in YOC’s work belongs to “on-off intermittency” [5–13]. However, there has been some confusion about this because YOC did not investigate the RZ map from the perspective of on-off intermittency. Indeed in the Letter [1] and subsequent review paper [2], they analyzed the RZ map by studying the largest Lyapunov exponent, the size of the snapshot attractor, and the simple one-dimensional contraction-expansion random map model to understand the intermittent transition behavior. But the essential geometrical structure related to the mechanism of on-off intermittency is absent in their analysis. Besides Heagy, Platt, and Hammel (HPH) commented that the snapshot attractor can undergo a form of intermittent behavior that is similar to on-off intermittency, but the size distribution of the snapshot attractor computed by YOC is quite different from the laminar phase distribution they obtained in their random walk model [14].

Meanwhile, Yang and Ding (YD) have studied a noise-driven uncoupled map lattice as a spatially extended system [15,16]. As a special case, they considered a map lattice where logistic map is located at each site un-

coupled with its neighbors and each map driven by a common random variable, which is regarded as a homogeneous background. In their work, similar transition which comes from the instability of the synchronous motion of the ensemble was found. However, on-off intermittency of the size evolution of the snapshot attractor was proposed merely on the ground of laminar distribution obtained from numerical calculations since YD were unable to map the size evolution of the snapshot attractor into a random walk. In this respect, their study was incomplete.

Recently synchronization in a pair of nonlinear systems subjected to the common noise is revisited [6,17–19]. Gade and Basu showed that this synchronization phenomena is indeed physical in certain cases, and for synchronization of those system the randomness is not vital [19]. Moreover we have shown that, in this kind of synchronization, the distribution of the random variable is vital and there exists on-off intermittency in the boundary of synchronization region [6]. Also the intermittent behavior of the size of snapshot attractor was discussed briefly. Note that synchronization of random dynamical systems have same meaning of the chaotic transition in YOC’s work. This notion of synchronization is analogous to the synchronization scheme* proposed by Pecora and Carroll, if we assume that random variable is realized by a system as a drive system and random dynamical systems are regarded as a response systems [20].

In this paper, we explicitly show that the size evolution of the snapshot attractor really has the structure of on-off intermittency contrary to the HPH’s comment. In

* The scheme is based on the fact that certain chaotic systems possess a self-synchronization property. A Chaotic system is self-synchronizing if it can be decomposed into subsystems: a drive subsystem and a stable response subsystem that synchronize when coupled with a common drive signal.

Section II, we briefly recapitulate the properties of the RZ map, and in Sec. II the mechanism of synchronization of two particles will be revealed by using the error dynamics. In Sec. III, we introduce modified definition of the size of the snapshot attractor for the case of ensemble of particles, and explicitly show that this modification leads to the structure of on-off intermittency. Finally we present summary and brief discussion in Sec. IV.

I. PROPERTIES OF THE RANDOM ZASLAVSKY MAP

A generic D -dimensional random map can be described as follow:

$$\mathbf{r}_{n+1} = \mathbf{F}_{\xi_n}(\mathbf{r}_n), \quad (1)$$

where $\mathbf{r}_n \in \mathbb{R}^D$ is column state vector and ξ_n is a random variable. So the map \mathbf{F}_{ξ_n} is chosen randomly at each iteration according to some rule generating ξ_n . As it was introduced in [1,2], the RZ map describes a particle floating on an incompressible fluid. There is constant divergence transverse to the surface, and this divergence leads to contraction on the surface. And there exists vortical flow with complicated time dependence. $\mathbf{r}_n = (x_n, y_n)^\top$ (the superscript ‘T’ means transpose operation) describes the position of a particle on the surface at $t = nT$, where T is a constant sampling time. \mathbf{F}_{ξ_n} is given by

$$\begin{aligned} x_{n+1} &= x_n + f(\alpha)y_n \bmod 2\pi \\ y_{n+1} &= g(\alpha)y_n + k \sin(x_{n+1} + \xi_n), \end{aligned} \quad (2)$$

where $f(\alpha) = (1 - e^{-\alpha})/\alpha$, $g(\alpha) = e^{-\alpha}$, and k and α are control parameters. In specific, α gives rate of constant contraction of surface, k stands for the parameter of vortical flow, x is angle variable, and y is radial variable. On the other hand, random variable ξ_n gives complicated time dependence of vortical flow, which represents fluid instabilities at low Reynolds numbers. When ξ_n is absent, Eq. (2) is often called the Zaslavsky map [21]. If we consider a strip $|y| > K_0$ where $K_0 > k(1 - e^{-\alpha})$, one iteration maps this strip into a narrow band $|y| < K_1 < K_0$. Thus long term behavior is confined to $|y| < k(1 - e^{-\alpha})^{-1}$. Note that Jacobian determinant of the map is $g(\alpha) = e^{-\alpha}$. Therefore, the map is contracting by the factor $g(\alpha)$ after each iteration. Given a uniform distribution of the ensemble of particles on the surface (two-dimension), we can find fractal distribution of particles for $\alpha < \alpha_c \approx 0.31$ after a few iteration. When we increase α close to α_c , snapshots show almost one-dimensional fractal structure (very thin line structure). And for the case of $\alpha > \alpha_c$, the snapshot collapses to a point (zero-dimension), and particles jump synchronously as if they were a single particle.

II. SYNCHRONIZATION OF TWO PARTICLES

From now on, we will consider the ensemble of particles which satisfy Eq. (2). Because ξ_n is describing geometry of vortical flow at $t = nT$ and particles are sprinkled on the surface, they have different initial conditions but feel common random driving ξ_n . To investigate the synchronization of particles, we will begin to study the dynamical behavior of two particles rather than the motion of whole ensemble of particles.

Let us consider a replica $\mathbf{r}'_n = (x'_n, y'_n)^\top$ which obeys the Eq. (2) as does \mathbf{r}_n . To show the mechanism of synchronization, we consider the error dynamics (ED) of this system, $\mathbf{e}_n = (u_n, v_n)^\top = \mathbf{r}'_n - \mathbf{r}_n$, which is the difference of two arbitrarily chosen particle’s positions. Then, the whole system $\mathbf{z}_n = (x_n, y_n, u_n, v_n)^\top$ can be described by

$$\begin{aligned} \mathbf{r}_{n+1} &= \mathbf{F}_{\xi_n}(\mathbf{r}_n), \\ \mathbf{e}_{n+1} &= \mathbf{G}_{\phi_n}(\mathbf{e}_n), \end{aligned} \quad (3)$$

where \mathbf{G}_{ϕ_n} is given by

$$\begin{aligned} u_{n+1} &= u_n + f(\alpha)v_n \bmod 2\pi \\ v_{n+1} &= g(\alpha)v_n + 2k \cos\left(\phi_n + \frac{u_{n+1}}{2}\right) \sin\left(\frac{u_{n+1}}{2}\right) \end{aligned} \quad (4)$$

with $[A \bmod B] \equiv (A + B/2 \bmod B) - B/2$ and $\phi_n \equiv x_{n+1} + \xi_n$. Here, we have applied mod operation according to the translational symmetry of u_n in trigonometric functions in Eq. (4). Note that the ED is driven by ϕ_n , which is the sum of x_{n+1} from $\mathbf{F}_{\xi_n}(\mathbf{r}_n)$ and random variable ξ_n . Therefore ϕ_n is not affected by the evolution of \mathbf{e}_n , and the transformed system have so-called skew-product structure mathematically [4]. Because the trajectory near hyperplane $\mathbf{e} = 0$ is governed by ϕ_n , we will study properties of the ED regarding the random dynamical variable ϕ_n as a system parameter ϕ which is constant during the evolution, before considering whole four-dimensional system.

A. Error Dynamics of two particles

We will investigate the local and global bifurcation structure by finding the fixed points of \mathbf{G}_ϕ and its phase portrait in order to reveal the underlying structure of the ED. When we impose condition $u_{n+1} = u_n$ and $v_{n+1} = v_n$ on \mathbf{G}_ϕ , $v_n f(\alpha)$ should be integer multiple of 2π . If $v_n = 0$,

$$\cos\left(\phi + \frac{u_n}{2}\right) \sin\left(\frac{u_n}{2}\right) = 0. \quad (5)$$

Then, there are two fixed points,

$$\mathbf{e}^* = \begin{pmatrix} u^* \\ v^* \end{pmatrix} = \begin{pmatrix} 0 \\ 0 \end{pmatrix} \quad \text{and}$$

$$\mathbf{e}^\circ = \begin{pmatrix} u^\circ \\ v^\circ \end{pmatrix} = \begin{cases} \begin{pmatrix} \pi - 2\phi \\ 0 \end{pmatrix} & \text{for } 0 \leq \phi < \pi \\ \begin{pmatrix} 3\pi - 2\phi \\ 0 \end{pmatrix} & \text{for } \pi \leq \phi < 2\pi. \end{cases} \quad (6)$$

Otherwise there is no fixed point, since $v_n f(\alpha)$ should be $\pm 2\pi, \pm 4\pi, \dots$. The \mathbf{e}_{n+1} near the fixed point \mathbf{e}^* is written as follows:

$$\mathbf{e}_{n+1} - \mathbf{e}^* = \mathbf{J}^*(\phi)(\mathbf{e}_n - \mathbf{e}^*) + \dots, \quad (7)$$

where $\mathbf{J}^*(\phi) = \frac{\partial \mathbf{G}_\phi}{\partial \mathbf{e}}|_{\mathbf{e}^*}$ is Jacobian matrix evaluated at \mathbf{e}^* . Two eigenvalues λ_+^*, λ_-^* and the corresponding eigenvectors $\mathbf{e}_+, \mathbf{e}_-$ can be obtained by solving eigenvalue problem of the matrix $\mathbf{J}^*(\phi)$. Pairs of eigenvalues give behavior along eigendirection of \mathbf{e}_\pm , and characterize the stability of \mathbf{e}^* [22]. From Eq. (4), Jacobian matrix is given by

$$\mathbf{J}^*(\phi) = \begin{pmatrix} 1 & f(\alpha) \\ k \cos \phi & g(\alpha) + kf(\alpha) \cos \phi \end{pmatrix}. \quad (8)$$

And its eigenvalues are

$$\lambda_\pm^* = \frac{1}{2} \{ 1 + g(\alpha) + kf(\alpha) \cos \phi \pm \sqrt{(1 + g(\alpha) + kf(\alpha) \cos \phi)^2 - 4g(\alpha)} \}. \quad (9)$$

Note that λ_\pm^* becomes unity for $\phi = \pi/2$ or $3\pi/2$ irrespective of α and k . In Fig. 1(b) the logarithm of $|\lambda_\pm^*|$ is plotted as a function of ϕ for $\alpha = 0.3$ and $k = 0.5$. We will use logarithms of eigenvalues as a measure of the stability of a fixed point. Stability along the eigendirection \mathbf{e}_+ changes at $\phi = \pi/2$ and $\phi = 3\pi/2$. For $\phi < \pi/2$ or $\phi > 3\pi/2$, the fixed point \mathbf{e}^* becomes a saddle point, at which trajectory is attracted along \mathbf{e}_- eigendirection and repelled along \mathbf{e}_+ eigendirection, since $\ln |\lambda_+^*| > 0$, $\ln |\lambda_-^*| < 0$ and λ_\pm^* is real. For $\pi/2 < \phi < 3\pi/2$ and $\ln |\lambda_+^*| < 0$, the region of ϕ is divided into two cases. First case is when logarithms of two eigenvalues are negative and different. In this region, \mathbf{e}^* become a stable node, which makes trajectories attracted along \mathbf{e}_+ to the fixed point, because $\ln |\lambda_+^*| < \ln |\lambda_-^*| < 0$. For the other case, when $\ln |\lambda_+^*| = \ln |\lambda_-^*| < 0$, two eigenvalues are complex conjugated pair whose absolute values are less than 1. Therefore, \mathbf{e}^* becomes a stable spiral (stable foci) and trajectory will be attracted to \mathbf{e}^* rotating around the fixed point.

Similarly for the other fixed point \mathbf{e}° , the Jacobian matrix is

$$\mathbf{J}^\circ(\phi) = \begin{pmatrix} 1 & f(\alpha) \\ -k \cos \phi & g(\alpha) - kf(\alpha) \cos \phi \end{pmatrix}, \quad (10)$$

and its eigenvalues are

$$\lambda_\pm^\circ = \frac{1}{2} \{ 1 + g(\alpha) - kf(\alpha) \cos \phi \pm \sqrt{(1 + g(\alpha) - kf(\alpha) \cos \phi)^2 - 4g(\alpha)} \}. \quad (11)$$

Same as the above case of \mathbf{e}^* , in Fig. 1(c) $\ln |\lambda_+^\circ|$ is zero at $\phi = \pi/2, 3\pi/2$ irrespective of α and k . However, the situation of stability is reversed. As shown in Fig. 1(b) and (c), \mathbf{e}^* becomes stable spiral or node(saddle) and \mathbf{e}° becomes saddle(stable spiral or node) at $\pi/2 < \phi < 3\pi/2$ ($0 < \phi < \pi/2$ or $3\pi/2 < \phi < 2\pi$). As a result Fig. 1(a) shows corresponding bifurcation diagram and \mathbf{e}^* and \mathbf{e}° exchange the stability through transcritical bifurcation at $\phi = \pi/2, 3\pi/2$ respectively. Note that \mathbf{e}^* is constant but changes its stability with the variation of ϕ .

For some value of ϕ close to $\pi/2$ or $3\pi/2$, an attracting closed orbit and a basin boundary between the stable fixed point and the closed orbit were found in the phase portrait. Indeed, we have obtained a homoclinic bifurcation which can be found in a dissipative pendulum with constant torque [23]. In our analysis, however, we have recognized that the existence of basin boundary as a result of global bifurcation does not affect our present results.

B. Synchronization and On-off Intermittency

Our main interest in this section is the mechanism of the synchronization of two particles. Therefore, we will return to Eq. (3), where ϕ_n changes for every iteration, and consider the stability of synchronized state based on the study of previous section. The synchronized state corresponds to \mathbf{e}^* in \mathbf{G}_{ϕ_n} . Because $\mathbf{e}^* = (0, 0)$ is a fixed point of \mathbf{G}_{ϕ_n} , trajectory starting from $\mathbf{z}_0 = (\mathbf{r}_0, \mathbf{e}^*)$ belongs to a class of a particular solution labelled by $(\mathbf{r}_0, \mathbf{e}^*)$ where \mathbf{r}_0 is an arbitrary chosen vector. This class of trajectories constitute 2-dimensional invariant subset \mathcal{M} embedded in the whole four-dimensional phase space. Because Eq. (3) contains random variable ϕ_n , it will fill the whole hyperplane satisfying $\mathbf{e} = \mathbf{e}^*$ and \mathcal{M} will be identical to the hyperplane. We say a subspace is *invariant* if a trajectory starting in the subspace always remains in the same subspace.

Let us consider a situation where a trajectory, which is initially located outside \mathcal{M} , and \mathbf{z}_n happens to be located in the vicinity of \mathcal{M} for some n . Whether \mathbf{z}_{n+1} will be attracted or repelled from \mathcal{M} is determined by the Jacobian matrix of subsystem \mathbf{G}_{ϕ_n} at \mathbf{e}^* given by Eq. (7). The Eq. (7) can be mapped into a random walk when we take logarithm of absolute value on each side of the equation as follows:

$$\ln |\mathbf{e}_{n+1}| = \ln |\mathbf{J}^*(\phi_n) \cdot \hat{\mathbf{e}}_n| + \ln |\mathbf{e}_n|. \quad (12)$$

Note that we have divided \mathbf{e}_n into $|\mathbf{e}_n|$ and unit vector $\hat{\mathbf{e}}_n = (\cos \theta_n, \sin \theta_n)^\top$, where $\theta_n = \tan^{-1}(v_n/u_n)$. Then, one can regard $\ln |\mathbf{e}_n|$ as n -th displacement of the random walk, and $\ln |\mathbf{J}^*(\phi_n) \cdot \hat{\mathbf{e}}_n|$ as its $n+1$ -th step width. Asymptotic behavior of the trajectory near \mathcal{M} is determined by the average of the step width, i.e., the bias of

random walk. This bias is called transverse Lyapunov exponent h_{\perp} , which measures global stability of \mathcal{M} , defined as

$$h_{\perp} = \int d\phi d\theta \rho(\phi, \theta) \ln |\mathbf{J}^*(\phi) \cdot \hat{\mathbf{e}}(\theta)|, \quad (13)$$

where $\rho(\phi, \theta)$ is probability distribution of ϕ and θ .

If $h_{\perp} < 0$, i.e., the average of step width is negative, the displacement of the random walk will decrease in time, and $|\mathbf{e}_n|$ will approach to zero in proportion to $e^{nh_{\perp}}$. Therefore \mathcal{M} is transversely stable, and the whole trajectories, which initially start from outside of \mathcal{M} , will be attracted to \mathcal{M} asymptotically. If $h_{\perp} > 0$, the small distance between the trajectory and \mathcal{M} will increase exponentially and at last will be affected by nonlinear term, which will reinject the trajectory to the neighborhood of \mathcal{M} . In this case \mathcal{M} is called transversely unstable. The transition from the former case to latter one according to the variation of system parameter has been investigated by others, and is called “blow-out” bifurcation [24–26].

Practically we can calculate h_{\perp} as follows:

$$\begin{aligned} e^{nh_{\perp}} &= \lim_{n \rightarrow \infty} \frac{\sqrt{u_n^2 + v_n^2}}{\sqrt{u_0^2 + v_0^2}} \\ &= \lim_{n \rightarrow \infty} |\mathbf{J}^*(\phi_n) \mathbf{J}^*(\phi_{n-1}) \cdots \mathbf{J}^*(\phi_0) \cdot \hat{\mathbf{e}}_0| \\ \rightarrow h_{\perp} &= \lim_{n \rightarrow \infty} \frac{1}{n} \sum_i \ln |\mathbf{J}^*(\phi_i) \cdot \hat{\mathbf{e}}_i|. \end{aligned} \quad (14)$$

The result h_{\perp} is shown in the Fig. 2 which coincides with the previous work [1,2].

It is also known that when h_{\perp} is slightly positive, some dynamical variables of the system can exhibit an extreme type of temporal intermittent bursting behavior: on-off intermittency [14,27]. The essential ingredients of on-off intermittency are : (a) a hyperplane should contain invariant subset and (b) trajectory near hyperplane shows additive random walk in log domain depending on the local stability of hyperplane along the transversal direction of \mathcal{M} [7,27]. Trajectory in large negative value in log domain will be shown approximately a constant in real scale, and corresponds to the ‘off’ state. In other case positive or small negative value in log domain corresponds to ‘on’ state. In the pairs of particles, we have shown that \mathcal{M} is the hyperplane containing invariant subset, and $\ln |\mathbf{e}_n|$ exhibits random walk near \mathcal{M} according to the stability of \mathbf{J}^* . Therefore we can conclude that there exists on-off intermittency. On the other hand, according to a result based on the study of a random walk, it is known that the probability of laminar length(L) is proportional to $L^{-3/2}e^{-L/L_s}$, where L_s is the length at which the systematic drift due to the bias and the diffusion spread of random variable without bias become comparable [5,7,14]. Fig. 3 shows characteristic scaling of on-off intermittency which $P(L)$ scales as $L^{-\frac{3}{2}}$.

In this section, we have shown the mechanism in the synchronization of two particles using skew-product

structure and stability analysis of \mathcal{M} and verified structure of on-off intermittency.

III. SYNCHRONIZATION OF ENSEMBLE OF N PARTICLES

In this section, we will study the behavior of ensemble of N particles. As described in previous section, on-off intermittency can be characterized by a biased random walk. To establish the link with a random walk with the size evolution of the snapshot attractor, let us consider the relation between the ED and the size of the snapshot attractor. YOC considered the size of the snapshot attractor S_n as the *rms* (root mean square) value of distance from the center of ensemble as follows:

$$S_n = \sqrt{\frac{1}{N} \sum_{i=1}^N (y_n^i - \bar{y}_n)^2}, \quad (15)$$

where y_n^i are coordinates of i -th particle ($i = 1, 2, \dots, N$) and $\bar{y}_n = N^{-1} \sum_i y_n^i$. However, \bar{y}_n is not so good choice to establish the random walk relation between S_n and S_{n-1} . Since \bar{y}_n is defined as sum of y_n^i and S_n^2 can be expressed by \bar{y}_n and average of $(y_n^i)^2$, then it is not trivial to consider limiting case of $S_n \rightarrow 0$. In order to use the result from the previous section, we consider the modified measure \tilde{S}_n which is the average length not from the center of the ensemble \bar{y}_n but from an arbitrarily chosen reference particle position y_n^r in the ensemble. Our modified measure is defined as

$$\tilde{S}_n = \sqrt{\frac{1}{N} \sum_i (y_n^i - y_n^r)^2} = \sqrt{\frac{1}{N} \sum_i (v_n^i)^2}, \quad (16)$$

which is *rms* distance in y direction, where $v_n^i = y_n^i - y_n^r$. The behavior of S_n and \tilde{S}_n can be seen in Fig. 4 for the case $N = 1000$, $\alpha = 0.3$, and $k = 0.5$. Fig. 4(b) shows the amplitude are slightly different, but bursting and laminar behaviors coincide. Moreover, as shown in Fig. 4(a), as S_n approaches to 0, \tilde{S}_n becomes identical to S_n . Therefore \tilde{S}_n may be replaced with S_n when one investigates the size of the snapshot attractor near synchronization transition point. Since our measure \tilde{S}_n can be decomposed into *rms* value of the ED variable v_n^i , the relation between \tilde{S}_{n+1} and \tilde{S}_n can be obtained from the relation between v_{n+1} and v_n . In the measure of \tilde{S}_n , the existence of the hyperplane containing invariant set is guaranteed by invariant hyperplane of two particles system, that is the hyperplane stands for the state when all the particles jump synchronously.

A. Uncoupled map lattice with homogeneous background

We analyzed one dimensional simple case of globally coupled logistic maps which was studied by YD [15,16].

Let us consider the system of N particles. They are located at y_n^1, \dots, y_n^N , and their dynamics are described by

$$y_{n+1}^i = z_n y_n^i (1 - y_n^i), \quad (17)$$

where $z_n = a\xi_n + b$ and ξ_n is a random variable uniformly distributed in the interval $(0, 1]$. Note that this system is identical to the model studied by HPH [14] to explain on-off intermittency. When $a = 1$ is fixed and b is varied, they reported that the transition from non-synchronous state to synchronous one is found at $b_c = 2.82$, and when $b > b_c$, the size evolution of the snapshot attractor exhibit on-off intermittency. We will explain this transition behavior with our measure \tilde{S}_n and the ED. If we consider the difference v_n^i between y_n^i and y_n^r such that

$$\begin{aligned} v_{n+1}^i &= y_{n+1}^i - y_{n+1}^r \\ &= z_n v_n^i (1 - 2y_n^r - v_n^i), \end{aligned} \quad (18)$$

then,

$$\begin{aligned} \tilde{S}_{n+1}^2 &= \frac{1}{N} \sum_{i=1}^N (v_{n+1}^i)^2 \\ &= \frac{1}{N} \sum_{i=1}^N z_n^2 (v_n^i)^2 (1 - 2y_n^r - v_n^i)^2. \end{aligned} \quad (19)$$

If we consider the limit $v_n^i \rightarrow 0$ and neglect higher order terms $\sum_i (v_n^i)^3$ and $\sum_i (v_n^i)^4$ near the transition region, Eq. (19) becomes $\tilde{S}_{n+1} \approx |z_n(1 - 2y_n^r)| \tilde{S}_n$. Then, we have obtained the following relation by taking logarithm on both side.

$$\ln \tilde{S}_{n+1} = \ln |z_n(1 - 2y_n^r)| + \ln \tilde{S}_n. \quad (20)$$

This relation can be interpreted such that the size evolution of the snapshot attractor in log domain is governed by the random walk with a step size $\ln |z_n(1 - 2y_n^r)|$. Similarly to Eq. (13) the transverse Lyapunov exponent is

$$h_\perp = \int dy \rho(z, y) \ln |z(1 - 2y)|, \quad (21)$$

where $\rho(z, y)$ is invariant probability density. This leads to the same transition point which is calculated by YD. One should notice that the random variable is multiplied *commonly* to every particles in the summation of Eq. (19), and this leads to on-off intermittency of \tilde{S}_n .

B. RZ map

In the case of the RZ map, we consider the case of $v_n^i \approx 0$. From Eq. (4),

$$\begin{aligned} v_{n+1}^i &= g(\alpha)v_n^i + 2k \cos(\phi_n + 0.5u_{n+1}^i) \sin(0.5u_{n+1}^i) \\ &= g(\alpha)v_n^i + 2k \cos \phi_n \sin[(\cot \theta_n^i + f(\alpha))v_n^i] \\ &\quad - k \sin \phi_n \sin^2[0.5(\cot \theta_n^i + f(\alpha))v_n^i] \\ &\approx [g(\alpha) + 2k \cos \phi_n (\cot \theta_n^i + f(\alpha))]v_n^i + O((v_n^i)^2), \end{aligned} \quad (22)$$

where $\cot \theta_n^i = u_n^i/v_n^i$ and $u_{n+1}^i = [\cot \theta_n^i + f(\alpha)]v_n^i$. Therefore,

$$\begin{aligned} \tilde{S}_{n+1}^2 &= \frac{1}{N} \sum_i [v_{n+1}^i]^2 \\ &\approx \frac{1}{N} \sum_i \{g(\alpha) + 2k \cos \phi_n [\cot \theta_n^i + f(\alpha)]\}^2 (v_n^i)^2 \\ &\quad + \frac{1}{N} \sum_i O[(v_n^i)^4]. \end{aligned} \quad (23)$$

Then, Eq. (23) have different result comparing with previous case, because the summation in Eq. (23) does not have a common driving. As a result, it seems that one could not deduce \tilde{S}_n from the right side. However, we have recognized the crucial property that the value of $\cot \theta_n^i$ for all i becomes identical when $v_n^i \approx 0$. That means that the whole particles aligned in a line passing through reference particle, because $\tan \theta_n^i$ is the slope of a line connecting position of the reference particle to that of the i -th particle. In Sec. II, we have shown that \mathbf{e}^* becomes a saddle or a spiral for most ϕ . When \mathbf{e}^* is saddle, particles are repelled along unstable direction. However, since $|\ln |\lambda_+^*|| < |\ln |\lambda_-^*||$, particles are attracted fast along \mathbf{e}_- and repelled slowly along \mathbf{e}_+ . Therefore, particles are scattered around along unstable eigendirection after a few iteration, and become a narrow stripe along a straight line from the reference particle. When \mathbf{e}^* is spiral, we have shown that the particles around \mathbf{e}^* rotate around the fixed point without changing the shape of distribution. Fig. 5 shows the behavior of particles near \mathbf{e}^* for constant ϕ when \mathbf{e}^* is saddle or spiral. After particles are scattered along a line, the Jacobian matrix maps the line passing through the position of reference particle to another line passing through that of reference particle. Therefore, we could approximate $\cot \theta_n = \cot \theta_n^1 = \cot \theta_n^2 = \dots = \cot \theta_n^N$ for $\tilde{S}_n \approx 0$. This fact is consistent with the finding of YOC that Lyapunov dimension becomes unity on chaotic side of transition. This represents that ensemble of N particles is embedded in one-dimensional manifold. Also from an evolution of uniformly distributed ensemble, we have found that near the fixed point all the particles are aligned in a line from the position of reference particle as shown in Fig. 6. Therefore, we can write as follow:

$$\tilde{S}_{n+1} = |g(\alpha) + 2k \cos \phi_n (\cot \theta_n + f(\alpha))| \tilde{S}_n. \quad (24)$$

By taking logarithm on both side, we find

$$\ln \tilde{S}_{n+1} =$$

$$\ln |g(\alpha) + 2k \cos \phi_n (\cot \theta_n + f(\alpha))| + \ln \tilde{S}_n. \quad (25)$$

As a result, Eq. (25) shows a random walk process in log domain. The transition point of the size of the snapshot attractor is same as that of two particles because the step size of \tilde{S}_n in Eq. (24) is same as that of v_n^i in Eq. (22). Furthermore, in the plot of laminar distribution of \tilde{S}_n ,

the distribution is not affected by the number of particles and shows same scaling of the two particles case, as depicted in Fig. 7, which shows the consistency of our results.

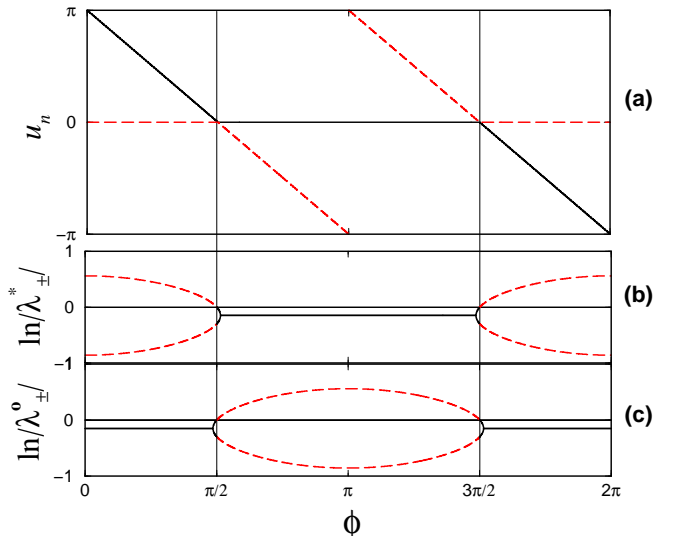
IV. SUMMARY AND DISCUSSION

In this paper, we have considered the mechanism of synchronization in random dynamical system. As a specific example, we have investigated the random Zaslavsky map in detail. From the ED of two particles, we have studied the bifurcation structure of invariant manifold and found transcritical bifurcation between saddle and stable node. Our results are consistent with those of YOC, but are more explicit in the perspective of on-off intermittency structure. In case of ensemble of many particles in the random Zaslavsky map, the long standing problem to map the size evolution of the snapshot attractor into a random walk is at last resolved by exploiting our modified definition of the size of the snapshot attractor, which is slightly different from the previously proposed one. From this success of mapping into a random walk, we have obtained qualitative understanding why this manifestation of intermittency has the same critical exponent, which is found from numerical simulation as that of the typical on-off intermittency. We emphasize that this mapping becomes possible when the ED variable are distributed on a line along the unstable direction of saddle. For further investigation, it will be interesting to study the other systems, that seem to be difficult to map into the form of a random walk.

ACKNOWLEDGMENTS

We thank P. Kang for valuable discussion. This work was supported by Creative Research Initiatives of the Korean Ministry of Science and Technology. Two of us (I. K. & Y.-J. P.) acknowledge support from the Ministry of Education, BK21 Project No. D-1099.

- [4] N. Platt, E. A. Spiegel, and C. Tresser, Phys. Rev. Lett. **70**, 279 (1993)
- [5] H. L. Yang and E. J. Ding, Phys. Rev. E **54**, 1361 (1996)
- [6] S. Rim, D.-U. Hwang, I. Kim and C.-M. Kim, Phys. Rev. Lett. **85**, 2304 (2000)
- [7] M. Ding and W. Yang, Phys. Rev. E **52**, 207 (1995)
- [8] Y.-C. Lai, Phys. Rev. E **53**, R4267 (1996)
- [9] M. Ding and W. Yang, Phys. Rev. E **56**, 4009 (1997)
- [10] Y.-C. Lai, Phys. Rev. E **54**, 321 (1996)
- [11] Z. Qu, F. Xie and G. Hu, Phys. Rev. E **53**, R1301 (1996)
- [12] A. Stefański, T. Kapitaniak, J. Brindley, and V. Astakhov, Phys. Rev. E **57**, 1175 (1998)
- [13] W.-H. Kye and D. Topaj, Phys. Rev. E **63**, 045202 (2001)
- [14] J. F. Heagy, N. Platt, and S. M. Hammel, Phys. Rev. E **49**, 1140 (1994)
- [15] H. L. Yang, and E. J. Ding, Phys. Rev. E **50**, R3295 (1994)
- [16] H. L. Yang, Z. Q. Huang, and E. J. Ding, Phys. Rev. E **54**, 3531 (1996)
- [17] S. Fahy, and D. R. Hamman, Phys. Rev. Lett. **69**, 762 (1992)
- [18] A. Maritan, and J.R. Banavar, Phys. Rev. Lett. **72**, 1451 (1994)
- [19] P. M. Gade, and C. Basu, Phys. Lett. A **217**, 21 (1996)
- [20] L. M. Pecora, and T. L. Carroll, Phys. Rev. Lett. **64**, 821 (1990)
- [21] G. M. Zaslavsky, Phys. Lett. A **69**, 145 (1978)
- [22] F. C. Moon, *Chaos and Fractal Dynamics: An Introduction for Applied Scientists and Engineers* (John Wiley & Sons, New York, 1992)
- [23] J. Guckenheimer and P. Holmes, *Nonlinear Oscillations, Dynamical Systems, and Bifurcations of Vector Fields* (Springer-Verlag, New York, 1983); see sec. 4.7
- [24] E. Ott, and J. C. Sommerer, Phys. Lett. A **188**, 39 (1994)
- [25] P. Ashwin, J. Buescu, and I. Stewart, Phys. Lett. A **193**, 126 (1994)
- [26] Y. C. Lai and C. Grebogi, Phys. Rev. E **52**, R3313 (1995).
- [27] N. Platt, S. M. Hammel, and J. F. Heagy, Phys. Rev. Lett. **72**, 3498 (1994)



E-mail addresses

a : zzamong@physics3.sogang.ac.kr
b : ibkim@physics3.sogang.ac.kr
c : rim@phys.paichai.ac.kr
d : chmkim@mail.paichai.ac.kr
e : yjpark@ccs.sogang.ac.kr

- [1] L. Yu, E. Ott, and Q. Chen, Phys. Rev. Lett. **65**, 2935 (1990)
- [2] L. Yu, E. Ott, and Q. Chen, Physica D **53**, 102 (1991)
- [3] F. J. Romeiras, C. Grebogi, and E. Ott, Phys. Rev. A **41**, 784 (1990)

FIG. 1. (a) Bifurcation diagram of the ED. In this figure v_n is omitted because fixed point is always 0. Horizontal axis is ϕ and its value is same as in (b) and (c). In the diagram, solid and dashed lines stand for stable and unstable fixed points respectively. (b) and (c) show logarithm of eigenvalues ($\lambda_{\pm}^*, \lambda_{\pm}^{\circ}$) of Jacobian matrix at \mathbf{e}^* and \mathbf{e}° , respectively. Vertical lines at $\phi = \pi/2, 3\pi/2$ stand for transition points of fixed points where $\ln |\lambda_{\pm}^*|$ and $\ln |\lambda_{\pm}^{\circ}|$ become 0.

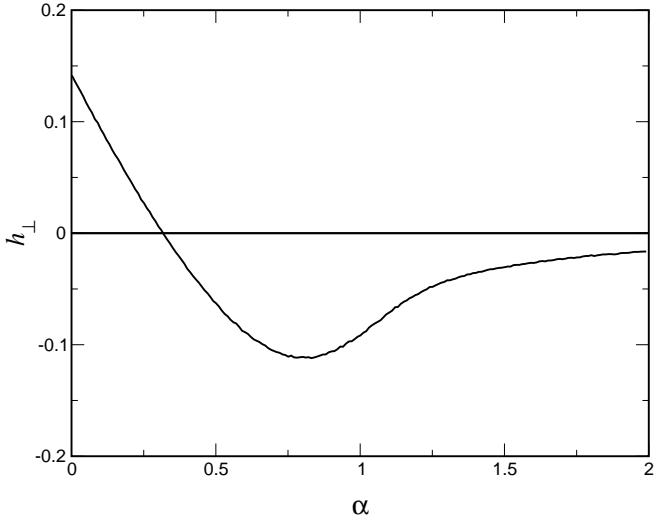


FIG. 2. h_{\perp} vs α when $k=0.5$.

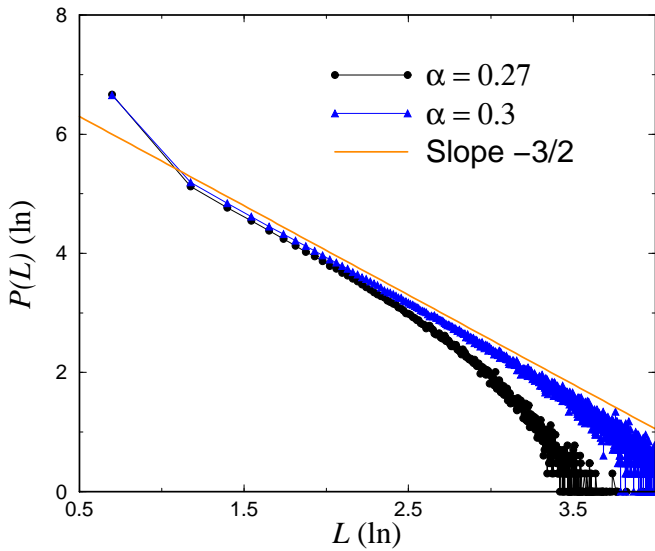


FIG. 3. Laminar distribution for two particles. Horizontal axis is length of laminar in logarithmic scale. Vertical axis is logarithm of probability of laminar length in arbitrary units. Filled circle means probability for $\alpha = 0.27$ and filled triangle for $\alpha = 0.3$. Gray straight line have $-3/2$ slope. The case of $\alpha = 0.27$ shows exponential shoulder which is typically shown in on-off intermittency models.

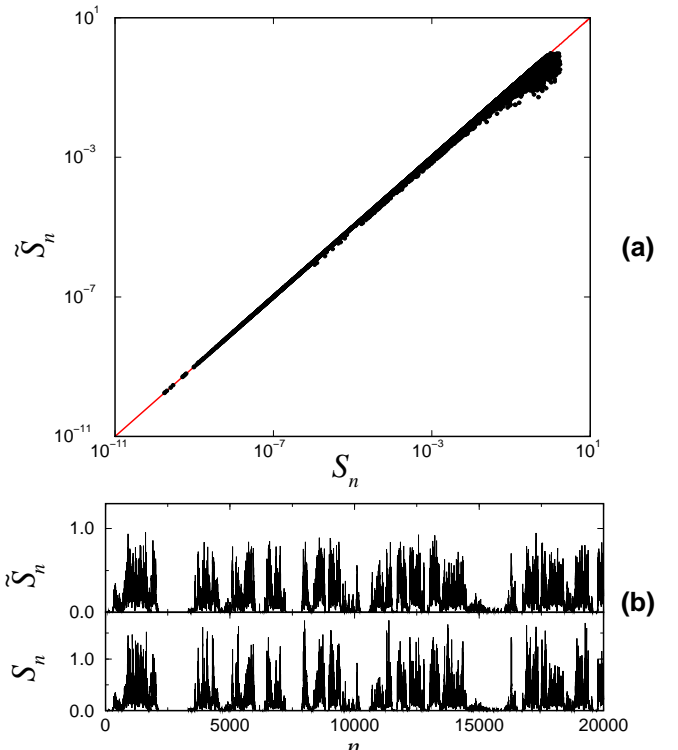


FIG. 4. (a) Horizontal and vertical axis are S_n and \tilde{S}_n in logarithmic scale, respectively. Both axes are logarithmic scale. Solid dots are data from 1000 particles when $\alpha = 0.3$ and grayed line is diagonal line. Data close to zero lies on the diagonal line and that means S_n and \tilde{S}_n become identical. (b) shows time series of S_n and \tilde{S}_n for same period. Although amplitudes are slightly different each other, timings of bursting and laminar period coincide.

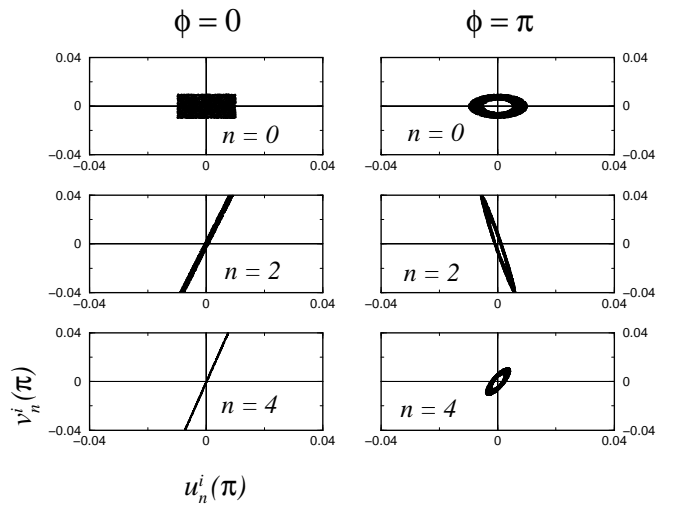


FIG. 5. Evolution of ensemble of 5000 particles for constant ϕ when $\alpha = 0.3$ and $k = 0.5$. Left column of three graphs are initial evolution of ensemble with $\phi = 0$, where fixed point at \mathbf{e}^* is saddle. We start with random initial points distributed within $-0.05\pi < u_0 < 0.05\pi$ and $0.1 < v_0 < 0.2$ uniformly in order to show the behavior near saddle. From upper to lower graphs, shape of ensemble stretch along unstable manifold as time flows. Contrast to left ones, right column are that of ensemble when $\phi = \pi$ and fixed point is spiral. The initial distribution rotate around origin with contracting its area. Note that in these graphs coordinates are u_n^i and v_n^i , i.e. relative displacement from the reference particle.

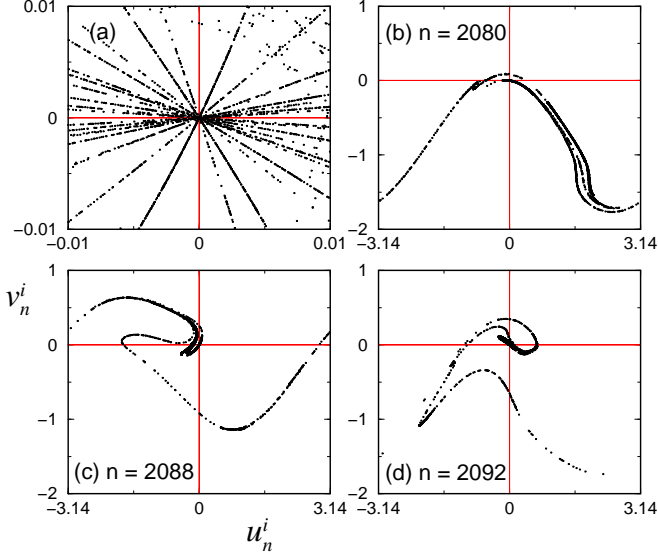


FIG. 6. Snapshot of 5000 particles when $\alpha = 0.3$ and $k = 0.5$. Initially, particles are distributed in the region $-0.5 < u_0 < 0.5$ and $-0.5 < v_0 < 0.5$. (b),(c) and (d) shows a fractal distribution of particles when $n = 2080, 2088$ and 2092 respectively. (a) shows small area of snapshot attractor for $n = 2080, 2081, \dots, 2099$ in a same graph. In this region particles are aligned in a line for each instant time when particle are close to origin. Each line stands for a snapshot for a given instant time. Note that in these graphs coordinates are u_n^i and v_n^i , i.e. relative displacement from the reference particle.

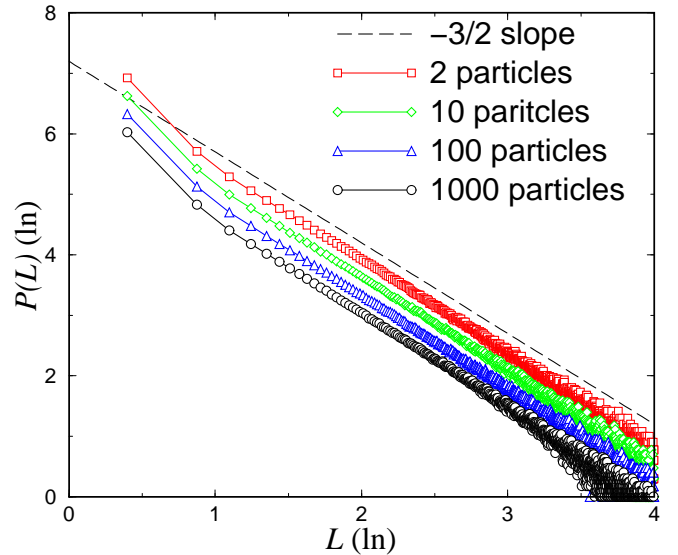


FIG. 7. Probability distribution $P(L)$ of laminar length L when $\alpha = 0.3$ and $k = 0.5$. We choose the threshold of on event as 10^{-4} . The unit of probability is arbitrary.